CESifo WORKING PAPERS

10037
2022

October 2022

Cities in a Pandemic: Evidence from China

Badi H. Baltagi, Ying Deng, Jing Li, Zhenlin Yang

CESifo

Impressum:

CESifo Working Papers
ISSN 2364-1428 (electronic version)
Publisher and distributor: Munich Society for the Promotion of Economic Research - CESifo GmbH
The international platform of Ludwigs-Maximilians University's Center for Economic Studies and the ifo Institute
Poschingerstr. 5, 81679 Munich, Germany
Telephone +49 (0)89 2180-2740, Telefax +49 (0)89 2180-17845, email office@cesifo.de
Editor: Clemens Fuest
https://www.cesifo.org/en/wp
An electronic version of the paper may be downloaded
· from the SSRN website: www.SSRN.com
· from the RePEc website: www.RePEc.org
· from the CESifo website: https://www.cesifo.org/en/wp

CESifo *Working Paper No. 10037*

Cities in a Pandemic: Evidence from China

Abstract

This paper studies the impact of urban density, city government efficiency, and medical resources on COVID-19 infection and death outcomes in China. We adopt a simultaneous spatial dynamic panel data model to account for (i) the simultaneity of infection and death outcomes, (ii) the spatial pattern of the transmission, (iii) the inter-temporal dynamics of the disease, and (iv) the unobserved city- and time-specific effects. We find that, while population density increases the level of infections, government efficiency significantly mitigates the negative impact of urban density. We also find that the availability of medical resources improves public health outcomes conditional on lagged infections. Moreover, there exists significant heterogeneity at different phases of the epidemiological cycle.

JEL-Codes: R100, R500, I180.

Keywords: Covid-19, urban density, government efficiency, cities.

Badi H. Baltagi
Department of Economics and Center for Policy Research, Syracuse University
USA – Syracuse, NY 13244-1020
bbaltagi@maxwell.syr.edu

Ying Deng
School of International Trade and Economics
University of International Business and Economics
China – Chaoyang District, Beijing 100029
ydeng@uibe.edu.cn

Jing Li
School of Economics
Singapore Management University
Singapore 178903
lijing@smu.edu.sg

Zhenlin Yang
School of Economics
Singapore Management University
Singapore 178903
zlyang@smu.edu.sg

October 13, 2022

1. INTRODUCTION

Density has advantages as well as disadvantages. If two people are close enough to exchange ideas face to face, they are also close enough to contract a contagious disease. This downside of cities was an imminent concern of city governance at the outbreak of the current COVID-19 pandemic. However, tracing the severity of the epidemic over time as it rampages worldwide, big cities do not necessarily suffer the most in terms of both infections and mortalities. This observation raises the question of what counteracting forces might mitigate potential public health consequences of urban density. In this paper, we argue that government management efficiency serves as a critical counteracting force that significantly reduces and, in China's case, even offsets the direct cost of city density in a pandemic. This aspect, however, has not been quantified carefully in the literature assessing the cost and benefit of cities.

In this paper, we study the roles of city density, city government efficiency, and medical resources in the context of early COVID-19 transmissions in China. The analysis draws on panel data of infections and subsequent deaths in 330 cities in China. The sample spans the period of the first epidemiological cycle between January 20, 2020, and March 31, 2020. We adopt a spatial dynamic panel data model to account for the nature of the spatial transmission and inter-temporal dynamics of the disease. We also account for correlations between infections and deaths by estimating a simultaneous spatial dynamic panel data model. By interacting lagged prevalence of the disease with time-invariant city characteristics, we uncover the role of city-specific features in altering the transmission speed at different phases of the epidemiological cycle. We find a large and significant role of urban density in contributing to high infections, especially at the early stage of the transmission cycle. We also document an important counteracting role of government efficiency and medical resources in reducing infections and mortality.

The findings in this paper contribute to the understanding of the "demons of density" manifested through issues related to public health (Glaeser, 2011). Urban economists have long been concerned with the easy spread of contagious diseases in cities as a type of urban cost. In the past, Plague, Cholera, and AIDS have caused several serious episodes of epidemics that affected urban areas more than rural areas. With the development of new technology and improved livelihood infrastructure, the urban population now in general enjoys higher life expectancy than their rural counterparts.

[1] However, these technologies do not immune cities from new outbreaks and the spread of new contagious air-borne diseases. Despite the intuition on the role of urban density in the transmission of these diseases, we lack rigorous evidence on the magnitude to which density and urbanization cause severe disease outbreaks and direct economic losses. This article contributes to this literature.

It is equally important to study the role of city government capacity and efficiency in fighting against the pandemic. A similar but broader notion of state capacity has been well recognized in the literature, especially in its role in driving nationwide economic prosperity (Acemoglu et al., 2015, 2016). How government capacity matters for cities, in particular, becomes critical, especially in a state of declared disaster with massive negative externalities, such as a pandemic.[2] How quickly public health measures are taken, how fast COVID-19 testing is adopted, how well contact tracing is administered, and how efficiently medical resources and vaccinations are deployed all matter critically in deterring rapid virus

[1] Improved water sanitation systems in cities are believed to be a key factor in improving urban health (Troesken, 2002; Cutler and Miller, 2005; Ashraf et al., 2016).

[2] All fifty states in the U.S. were under a major disaster declaration by April 13, 2020 due to the failure in containing early-stage COVID-19 transmissions.

transmissions and reducing death tolls.[3] The effective enforcement of these control measures depends on government efficiency, which echoes the notion of state capacity in the economics literature and the call for "a strong state" in combating the crisis in media coverage.[4] We demonstrate that there are significantly fewer COVID-19 cases in cities with more effective governments, which highlights the importance of city government capacity in combating the epidemic.

We also study the role of medical resources to provide a fuller picture of cities fighting against the pandemic. It is widely documented that medical resources are highly concentrated in large cities (Li, 2014). The availability of medical services allows sick patients to receive necessary medical treatment and improves their chances of survival. In other words, although city density imposes a high risk of infection due to intimate social contact and interactions, abundant medical resources available in large cities help mitigate the cost of infection by improving the chance of survival. This aspect is also crucial in assessing the net cost of urban density amid the global pandemic.

Studying these issues in the context of early COVID-19 transmissions in China yields several advantages for our empirical design. First, China completed the full cycle of its first-

[3] For instance, Lee and Lee (2021) and Argente et al. (2022) demonstrate that effective public disclosure of COVID-19 cases' residences and their mobility paths dramatically affects location-specific mobility patterns and the subsequent infection and death outcomes. We consider this as one of the channels through which government efficiency impacts public health outcomes.

[4] In the literature, state capacity is shown to be vital for economic development. There are, however, few studies linking state capacity to its effectiveness in pandemic control, despite heated discussions in the media in response to the U.S. failure to control the virus (Leonhardt, 2020; Crow and Kuchler, 2020; Krugman 2020). Narita and Sudo (2021) highlight the role of different political regimes in impacting the economic performance and public health outcomes during COVID-19 and, in particular, link a stronger democracy to weaker and narrower containment policies as a key mechanism. In comparison, our paper presents a narrower and a more direct focus on local government capacity.

round anti-corona virus campaign during our sample period. Since the middle of March 2020, daily new cases in China have been reduced to near-zero levels. The completion of a cycle allows us to trace the full dynamics of the outbreak. Second, the early stage of COVID-19 is associated with a high death rate with no effective vaccination and treatment. This feature led to a strong emphasis on curbing disease transmissions. In addition, China's pandemic management follows a top-down approach in which the central government declares the zero-COVID policy, and the local government must treat the policy as a primary political task and a top objective of the country. Such a political regime, combined with the nature of the early phase of COVID-19, ensures the homogeneity in local government objectives and leaves the efficiency of management a key political factor driving the variation in the anti-corona virus campaign.[5] Third, China imposed a lockdown on Wuhan on January 23, 2020, to quarantine the epicenter of COVID-19. The lockdown effectively reduced infection cases outside Wuhan and allowed for local government measures to take effect (Fang et al., 2020).

We adopt a simultaneous spatial dynamic panel data model to account for various features associated with disease transmissions. The simultaneous structure of the infection and death equations allows us to model the death tolls conditional on lagged infections and address potential correlations in the corresponding error terms to achieve estimation efficiency. We also include a spatial autoregressive term to account for the cross-city transmission of the disease in our model. The spatial weight matrix is specified in various ways to capture the varying natures of cross-sectional dependence and to ensure the robustness of our estimates. The

[5] This feature allows us to identify the impact of government efficiency from various confounding factors related to ideology and formal or informal institutions, such as laws, forms of organization, social norms, trust in political institutions, etc, that impact human behaviors during a pandemic (Rodríguez-Pose and Burlina, 2021 and Narita and Sudo, 2021, Bottasso et al., 2022).

dynamic structure of the model further captures the inter-temporal dynamics of the virus transmission.

Despite the richness of the model, the system of equations suffers from three sources of endogeneity. First, there may exist city-specific or time-specific unobserved characteristics that are correlated with our key regressors. Second, the presence of time dynamic effects may induce endogeneity if the unobserved city-specific effects exist (random or fixed), see Baltagi (2021). Third, a reflection problem arises from the contemporaneous spatial lag effect.

To address the first endogeneity concern, we take advantage of the panel structure and control for two-way fixed effects which account for unobserved city-specific and time-specific characteristics. The second and third endogeneity concerns are addressed via an instrumental variables approach. The instruments for the time-lagged dependent variables are obtained within the system as explained in Section 3 in detail. In brief, we adopt a forward orthogonal deviations (FOD) transformation which conveniently leaves out the past values of the dependent variable as ideal sources of exogeneity in constructing instruments.[6] Meanwhile, the exogenous time-lagged dependent variables also serve as the source of exogeneity in constructing instruments for the contemporaneous spatial lag effect.

We obtain three main findings. First, we find strong correlations in the error terms of both infection and death equations, especially for the pre-peak period. The presence of correlations between infections and deaths calls for the estimation of a system of two equations to improve efficiency. Second, we document strong spatial dependence in the prevalence of COVID-19 infections. Direct and indirect effects are similarly strong in magnitude for the pre-peak period, but the direct effect dominates in the post-peak period. The evidence demonstrates the

[6] FOD is also known as the Helmert transformation which subtracts the average of all future observed values from the current value.

importance of cross-city collaboration in fighting against the pandemic, especially in the early phase of transmission. Third, we find that population density plays an important role in contributing to the level of new infections, but government efficiency significantly reduces the number of new infections. Both effects are strikingly more pronounced during the pre-peak period. We also find that the availability of medical resources improves public health outcomes conditional on lagged infection cases. This effect is slightly increased for the post-peak period, compared to the pre-peak period, showing improvement in medical effectiveness over time. The key findings are robust to a variety of specification checks that we perform in the paper.

The remainder of the paper is organized as follows. In Section 2, we discuss burgeoning literature linking city characteristics and other factors to within-city COVID-19 prevalence and cross-city virus transmission. Section 3 lays out our conceptual framework and empirical methodology. Section 4 presents data and variables. Section 5 shows the empirical results and robustness checks. Section 6 concludes.

2. LITERATURE

There is an emerging literature studying the relationship between population density and the prevalence of COVID-19 or pandemics in general. Wheaton and Thompson (2020a) study 372 CBSAs and 628 counties in the U.S. and find a significantly positive correlation between population density and the incidence of the disease. Wheaton and Thompson (2020b) further explore more-refined data at the level of municipalities and towns in Massachusetts, and document that greater density is associated with a significantly higher per capita incidence of the disease. Almagro and Orane-Hutchinson (2020) also find a positive relationship between population density and confirmed cases across New York City zip code areas and Desmet and Wacziarg (2020) show similar patterns across U.S. counties. Carozzi, Roth, and Provenzano

(2020) use instrumental variables based on historical information to address the potential endogeneity of urban density and obtain similar patterns.[7]

Overall, the evidence seems to suggest that high population density in urban areas impose inherent public health risks during a pandemic. Does this mean that cities unavoidably suffer from the spread of contagious diseases and there is no cure? To answer this question, we seek to understand the role of various other city-specific features that are either exogenously shaped or endogenously determined in general equilibrium but before the threat of a global pandemic. As the current pandemic is unprecedented in recent history and is unforeseen, we argue that other city-specific features that we observe before the pandemic are not developed in response to the potential threat of a large-scale spread of a contagious disease. Hence, the nature and the scale of the current pandemic allow us to causally evaluate the impact of various city-specific characteristics on the ongoing coronavirus spread.

Several papers study the severity of COVID-19 in relation to other aspects of cities. For example, Wheaton and Thompson (2020a) show that the share of land use in commercial-industrial categories is positively associated with high infection rates. Almagro and Orane-Hutchinson (2020) investigate the roles of city demographics such as race, income, and occupation. Desmet and Wacziarg (2020) examine the link between the severity of the outbreak and the roles of public transportation and political preference. Adda (2016) shows that the expansion of transportation networks increases the spread of the virus and has significant health

[7] Qiu, Chen, and Shi (2020) control for population density in explaining cross-city transmissions of COVID-19 in China. They instrument lagged infections with weather conditions and document a negative and close to zero effect of population density. Li and Ma (2020) also document a lack of correlation between population size and the number of local transmissions. However, both findings could be confounded by the omitted role of government efficiency emphasized in our paper. This point is also highlighted on Page 4 of Li and Ma (2020) that "the lack of correlation between population size and the number of local transmissions indicates the effectiveness of a range of public health interventions aimed at minimizing interpersonal contact."

costs. Glaeser, Gorback, and Redding (2020) highlight the importance of urban mobility in the spread of COVID-19.[8] Xie et al. (2021) document a negative relationship between the availability of public health resources and the mortality rate of the disease. In sum, the direct impact of urban density could be either aggravated or mitigated by other important city-specific features.

Besides focusing on city-specific features in driving the spread of COVID-19 within a city, existing studies also highlight the importance of cross-city contagion and its contributing factors. Li and Ma (2020) use a spatial general equilibrium model to evaluate the impacts of migration flows and transportation infrastructure on the cross-city transmission of COVID-19 in China. Kuchler et al. (2021) use aggregate data from Facebook to show that COVID-19 is more likely to spread between regions with stronger social network connections. Mangrum and Niekamp (2020) suggest that college student travel also contributed to the cross-city COVID-19 spread. It is, therefore, important to model cross-city transmissions when explaining the variation in the severity of city-specific outbreaks.

Recognizing the association between social mobility and the spatial spread of the disease both within and between cities, the literature on COVID-19 also evaluates the effectiveness of the policies imposing mobility and travel restrictions. For example, Greenstone and Nigam (2020), Dave et al. (2020), and Maloney and Taskin (2020) highlight the importance of social distancing. Brzezinski et al. (2020) evaluate the impact of government-ordered lockdowns. Chinazzi et al. (2020) use a global metapopulation disease transmission model to show that the travel quarantine of Wuhan had a marked effect on virus transmission on the international scale.

[8] Linking cell phone data to COVID-19 cases per capita and applying an instrumental variable approach, the paper documents a 20 percent decrease of total COVID-19 cases for every 10-percentage point fall in mobility.

Fang et al. (2020) employ a difference-in-differences strategy to show that the lockdown of Wuhan contributes significantly to reducing the total infection cases outside of Wuhan.

Our paper contributes to the literature by highlighting the role of a previously overlooked fundamental institutional force that governs the effectiveness of implementing relevant policies in combating COVID-19. We document the role of government efficiency in counteracting the negative impact of urban density on COVID-19 prevalence in China. The focus differs from Narita and Sudo (2021) that highlight the role of different political regimes. The paper also highlights the cross-city contagion of infections at different phases of the epidemiological cycle which provides empirical justification for a broad theoretical literature modeling the spatial diffusion of COVID-19 across countries or locations, see Antras, Redding, and Rossi-Hansberg (2020), Bisin and Moro (2020), and Cunat and Zymek (2020).

3. METHODOLOGY

Given the nature of the pandemic, we follow a spatial dynamic econometric modelling approach to model cross-city variation in infection and death outcomes in a simultaneous equations setting while controlling for potential spatial interactions and cross-sectional dependence.[9] The model is specified as follows:

$$\begin{aligned} Infection_{it} = {} & \beta_{11} \sum_{j=1}^{n} w_{ij} Infection_{jt} + \beta_{12} Infection_{i,t-1} \\ & + \beta_{13} Infection_{i,t-1} \times Density_i \\ & + \beta_{14} Infection_{i,t-1} \times Efficiency_i + \alpha_{1i} + \lambda_{1t} + u_{1,it}, \end{aligned} \tag{3.1}$$

[9] We focus on death outcomes as opposed to recovered cases because the criterion for recovery varies over time and across cities and death is less subject to measurement errors.

$$Death_{it} = \beta_{21} Infection_{i,t-1} + \beta_{22} Infection_{i,t-1} \times Beds_i + \alpha_{2i} + \lambda_{2t} + u_{2,it}, \tag{3.2}$$

where subscript $i = 1, 2, \ldots, n$ represents city and subscript $t = 1, 2, \ldots, T$ represents time. We simplify notation in Equations (3.1) and (3.2) by stacking observations over the city index, *i*, for each time period, t, and consider the following vector form for $t = 1, 2, \ldots, T$,

$$Infection_t = \beta_{11} WInfection_t + \beta_{12} Infection_{t-1} + \beta_{13} Infection_{t-1} \odot Density + \beta_{14} Infection_{t-1} \odot Efficiency + \alpha_1 + \lambda_{1t} l_n + u_{1t}, \tag{3.3}$$

$$Death_t = \beta_{21} Infection_{t-1} + \beta_{22} Infection_{t-1} \odot Beds + \alpha_2 + \lambda_{2t} l_n + u_{2t}, \tag{3.4}$$

where $Infection_t = (Infection_{1t}, \ldots, Infection_{nt})'$ and $Death_t = (Death_{1t}, \ldots, Death_{nt})'$ are $n \times 1$ vectors of newly reported infections and deaths for n cities at time t; $Density = (Density_1, \ldots, Density_n)'$, $Efficiency = (Efficiency_1, \ldots, Efficiency_n)'$, and $Beds = (Beds_1, \ldots, Beds_n)'$ are time-invariant $n \times 1$ vectors that represent city population density, government efficiency, and available medical resources; $\odot$ represents the Hadamard product (also known as the element-wise product); $\alpha_1 = (\alpha_{11}, \ldots, \alpha_{1n})'$ and $\alpha_2 = (\alpha_{21}, \ldots, \alpha_{2n})'$ are $n \times 1$ vectors of city fixed effects; W is a row-normalized $n \times n$ spatial weight matrix with the $(i, j)^{th}$ element represented by w_{ij}. λ_{1t} and λ_{2t} are time fixed effects with l_n being an $n \times 1$ vector of ones; $u_{1t} = (u_{1,1t}, \ldots, u_{1,nt})'$ and $u_{2t} = (u_{2,1t}, \ldots, u_{2,nt})'$ are $n \times 1$ vectors of remainder error terms.

The spatial structure is defined as follows. We start by capturing the spatial relationship based on the travel intensity between two cities. In the baseline specification, the pairwise travel intensity between two cities is calculated as the average travel intensity two weeks before the start of the sample. This is before the date when a top Chinese medical expert, Dr. Zhong

Nanshan, announced on state television that the virus is transmissible between people and, hence, captures the original mobility linkages between cities unaffected by potential fear to travel. As the spatial transmission of the disease is directly affected by mobility, the travel intensity before the Wuhan lockdown serves as an exogeneous but relevant measure to capture inherent spatial interactions between cities. In this case, a typical element w_{ij} of W is defined as the proportion of inbound travels into city i that come from city j.[10]

Next, we specify the error structure in the model. Note that u_{1t} is the error term for the infection equation and u_{2t} is that for the death equation. Their elements, $(u_{1,it}, u_{2,it})$, are allowed to be correlated within each pair (simultaneity) and are assumed to be independent and identically distributed (iid) across all pairs. Specifically, $(u_{1,it}, u_{2,it}),\ i = 1, \dots, n, t = 1, \dots, T$, are assumed to be $iid(0, \Sigma)$, where $\Sigma = \begin{pmatrix} \sigma_1^2 & \sigma_1\sigma_2\rho \\ \sigma_1\sigma_2\rho & \sigma_2^2 \end{pmatrix}$ with σ_1^2 and σ_2^2 being the variances of $u_{1,it}$ and $u_{2,it}$, and ρ being the correlation coefficient between $u_{1,it}$ and $u_{2,it}$.

While it is important to have the three effects (unobserved city and time heterogeneity, spatial interaction, and time dynamics) under control when studying the factors impacting the infection and death outcomes, these three effects are also the sources of endogeneity, making the model estimation and inference difficult. First, the unobserved city-specific or time-specific effects may be correlated with the key regressors arbitrarily. Hence, they must be treated as fixed parameters (or fixed effects). Joint estimation of these fixed effects together with the model's common parameters makes the estimates of (some) common parameters inconsistent or asymptotically biased, giving rise to the *incidental parameters problem* of Neyman and Scott (1948). The standard way of handling the fixed effects is to transform the model to wipe out these effects and then run an OLS on the transformed model. This method produces consistent

[10] We experiment with alternative ways of defining the spatial weight matrix in our robustness checks.

estimates for regression coefficients for panel data models with strictly exogenous regressors but not for models with weakly exogenous or endogenous regressors.

Second, the presence of time-lagged terms in addition to the city-specific effects introduces weak exogeneity (with respect to idiosyncratic errors) and endogeneity (with respect to the city-specific effects). This makes the standard panel estimation methods invalid whether the city-specific effects are treated as random or fixed effects.[11] To see this, consider the OLS estimation when city-specific effects are treated as random effects. The compound error term $\alpha_{1i} + u_{1,it}$ is correlated with the lagged dependent variable $Infection_{i,t-1}$ since $Infection_{i,t-1}$ also contains city-specific effects α_{1i}. This renders the OLS estimator inconsistent. When the within estimator is applied, the within transformation is employed to eliminate city fixed effects and then an OLS regression is run on the transformed model. The within transformation, however, introduces correlations between the demeaned lag dependent variable ($Infection_{i,t-1} - \overline{Infection}_{i,.}$) and the demeaned error term ($u_{1,it} - \bar{u}_{1,i.}$), leading to the inconsistency of the within estimator, which is the well-known Nickell (1981) bias.

Third, the inclusion of the contemporaneous spatial lag effect as a regressor induces endogeneity. That is, for city i, its neighbor's (say, city $j's$) infection outcome, $Infection_{jt}$, is adversely affected by city $i's$ outcome, hence $\sum_{j=1}^{n} w_{ij}\, Infection_{jt}$ is correlated with the error term $u_{1,it}$, causing standard panel estimation methods to be invalid.

From the above, one sees that the three types of endogeneity problems are not isolated and must be dealt with collectively. We rely on an instrumental variable approach following an FOD (forward orthogonal deviations) transformation. In particular, we obtain instruments that

[11] The presence of time lagged term and its interaction with time-invariant variables rule out the use of (quasi) likelihood type approach due to the unavailability of a proper likelihood function.

are based on exogenous regressors in previous periods through an FOD transformation as opposed to a within transformation to eliminate the city fixed effects. The difference between an FOD transformation and a within transformation is that the FOD transformation subtracts the mean of future values only, leaving out the current and past values, in computing the mean. This convenient feature provides an opportunity for the lagged values of the dependent variable to be used as instruments for the time dynamic terms (Lee and Yu, 2014).

The FOD transformation of a variable, say $Infection_t$, is defined simply as follows:

$$Infection_t^* = \sqrt{\frac{T-t}{T-t+1}}\Big(Infection_t - \frac{1}{T-t}\sum_{h=t+1}^{T} Infection_h\Big), \quad t = 1,2,\dots,T-1. \tag{3.5}$$

The transformed errors are thus $u_{rt}^* = \sqrt{\frac{T-t}{T-t+1}}(u_{rt} - \frac{1}{T-t}\sum_{h=t+1}^{T} u_{rh})$ for $r = 1, 2$. $Death_t^*$ is defined similarly. Due to the time-invariant nature of the variables $Density$, $Efficiency$ and $Beds$, the transformed interaction terms are simply $Infection_t^* \odot Density$, $Infection_t^* \odot Efficiency$ and $Infection_t^* \odot Beds$, $t = 1,\dots,T-1$.[12]

After the FOD transformation, Equations (3.3) and (3.4) become, for $t = 1,\dots,T-1$,

$$\begin{aligned} Infection_t^* = {} & \beta_{11} WInfection_t^* + \beta_{12} Infection_{t-1}^* \\ & + \beta_{13} Infection_{t-1}^* \odot Density \\ & + \beta_{14} Infection_{t-1}^* \odot Efficiency + \lambda_{1t}^* l_n + u_{1t}^*, \end{aligned} \tag{3.6}$$

[12] The FOD transformation is often referred to as Helmert's transformation in the literature. See for details Arellano and Bover (1995, p.41), and Cameron and Trivedi (2005, p.759)

$$Death_t^* = \beta_{21} Infection_{t-1}^* + \beta_{22} Infection_{t-1}^* \odot Beds + \lambda_{2t}^* l_n + u_{2t}^*. \qquad (3.7)$$

The advantages of the FOD transformation are seen immediately. First, it wipes out the unobserved city-specific effects and automatically adjusts the loss of degrees of freedom (the effective sample size is now $n(T-1)$).[13] Second, the transformed error pairs $(u_{1,it}^*, u_{2,it}^*)$ remain independent across i and uncorrelated over t with the same mean and variance as the original error pairs (as seen below).[14] Third, $Infection_{t-1}$ is correlated with $Infection_{t-1}^*$, but uncorrelated with u_{1t}^*, implying that $Infection_{t-1}$ is a valid instrument for $Infection_{t-1}^*$.[15]

Interestingly, the FOD transformation is related to the within transformation and is a special case of the general class of orthonormal transformations. Let $J_T = I_T - \frac{1}{T} l_T l_T'$ be the within transformation matrix, where l_T denotes a $T \times 1$ vector of ones. Let $(F_{T,T-1}, \frac{1}{\sqrt{T}} l_T)$ be the orthonormal matrix of the eigenvectors of J_T, where $F_{T,T-1}$ consists of eigenvectors corresponding to the $T-1$ unit eigenvalues. The within transformed variables are obtained through $[Infection_1, Infection_2, \ldots, Infection_T] J_T$, and the general orthonormal

[13] The first difference (FD) transformation shares the same property, but the within transformation does not. The time-specific effects can be removed by another transformation but given the fact that our time dimension is not big and that the analyses are done separately for before and after the peak of the pandemic, we simply control the time effects by adding the time dummies in the model.

[14] Under both FD and within transformations, the transformed error pairs remain independent across i but become correlated over t.

[15] The FD transformation can achieve the same goal as does the FOD transformation as far as finding instruments is concerned. Intuitively, FOD may perform better than FD as, e.g., $Infection_{t-1}$ may be 'stronger' when instrumenting for $Infection_{t-1}^*$ than for $\Delta\, Infection_t$ as in the former $Infection_{t-1}$ is the main term but in the latter the two terms have equal weights. Indeed, Hayakawa (2009) and Phillips (2019) find that the FOD transformation has better finite sample properties than the FD transformation.

transformed variables are obtained through $[Infection_1, Infection_2, \ldots, Infection_T]F_{T,T-1}$. The former is $n \times T$ and the latter is $n \times (T-1)$. If we write Equation (3.5) as $Infection_t^* = [Infection_1, Infection_2, \ldots, Infection_T]f_t^0$ where $f_t^0 = \sqrt{\frac{T-t}{T-t+1}}(0_{t-1}', 1, \frac{-1}{T-t}, \ldots, \frac{-1}{T-t})'$ and 0_{t-1} is a $(t-1) \times 1$ vector of zeros, and then define $F_{T,T-1}^0 = [f_1^0, f_2^0, \ldots, f_{T-1}^0]$, we see that $F_{T,T-1}^0$ is a special choice of $F_{T,T-1}$. An important property of the eigenvectors is that they are orthonormal, i.e., $F_{T,T-1}'F_{T,T-1} = I_{T-1}$. Therefore, $Var(u_{rt}^*) = \sigma_r^2 I_n$ for $r = 1, 2,$ and $cov(u_{1t}^*, u_{2t}^*) = \sigma_1\sigma_2\rho I_n$ if $t = s$; 0 if $t \neq s$.

In this new system of equations, the city fixed effects α_1 and α_2 are eliminated. The time fixed effects λ_{1t}^* and λ_{2t}^* are captured by time dummies. Because u_{1t}^* involves $(u_{1t}, u_{1,t+1}, \ldots, u_{1T})$ and $Infection_{t-1}^*$ involves $(Infection_{t-1}, Infection_t, \ldots, Infection_T)$ which depends on $(u_{1t}, u_{1,t+1}, \ldots, u_{1T})$, $Infection_{t-1}^*$ and u_{1t}^* are correlated. More generally, all the right-hand-side regressors of Equation (3.6) are correlated with their own error term u_{1t}^*. If u_{1t}^* and u_{2t}^* are correlated, the right-hand-side regressors of Equation (3.7) are correlated with the error term u_{2t}^* as well. This renders the OLS estimator biased and inconsistent.

Conveniently, the endogeneity in the transformed system of equations can be addressed by obtaining instruments within the system. The idea is that the original lagged outcome variables are not correlated with the transformed error terms but predict our key regressors. Therefore, they serve as ideal exogenous sources to help construct instruments. For example, we use $Infection_{t-1}$ as an instrument for $Infection_{t-1}^*$, since it is correlated with $Infection_{t-1}^*$ but not correlated with u_{1t}^*. Similarly, we use $Infection_{t-1} \odot X$ as instruments for $Infection_{t-1}^* \odot X$, where $X \in (Density, Efficiency, Beds)$.

The proposed instruments are also relevant when it comes to addressing the endogeneity problem arising from the contemporaneous spatial effect. The conventional instruments for the

spatial lagged dependent variable are the spatial lags of the exogenous regressors. According to Kelejian and Prucha (1998), the ideal instrument for $WInfection_t^*$ is $WE(Infection_t^*)$, where $E(Infection_t^*)$ depends on the exogenous regressors and their spatially weighted counterparts. In our model, however, all explanatory variables are endogenous and require instrumental variables. Therefore, $E(Infection_t^*)$ relies on the exogenous time-lagged dependent variable, $Infection_{t-1}$, its interactions with the exogenous city-specific indices, $Infection_{t-1} \odot X$, and their spatially weighted counterparts, $WInfection_{t-1}$ and $WInfection_{t-1} \odot X$. We use the spatial lags of all the above terms, $WInfection_{t-1}$, $WInfection_{t-1} \odot X$, $W^2Infection_{t-1}$, and $W^2Infection_{t-1} \odot X$, for $X \in (Density, Efficiency, Beds)$, to instrument for the contemporaneous spatial lagged dependent variable $WInfection_t^*$.[16]

We undertake a 3SLS approach suggested by Yang and Lee (2019) to estimate Equations (3.6) and (3.7). In the first stage, we regress each endogenous variable on all the proposed instruments to obtain its fitted value. In the second stage, we run an OLS with all the endogenous variables replaced by their fitted values from the first stage and generate 2SLS residuals. In the third stage, we run a GLS based on the variance co-variance matrix of the error terms estimated based on the 2SLS residuals to obtain 3SLS estimates for Equations (3.6) and (3.7).

4. DATA AND VARIABLES

We rely on a variety of data sources for our analysis. We first obtain daily city-level COVID-19 transmission records from the National Health Commission of China. The data

[16] We test for weak instruments based on the first stage regressions. All the specifications reject the null hypothesis of weak instruments. Since the number of instruments exceeds the number of endogenous regressors, we perform the Sargan-Hansen over-identification test for the infection equation and death equation separately. Both equations do not reject the null hypothesis of over-identification.

cover 330 cities within mainland China for the period between January 20 and March 31, 2020. Figure 1 reports the temporal and spatial patterns of the disease transmission. Panel A shows the daily new infection cases averaged across all cities. Since January 21, the virus spread quickly, and the average number of daily new inflections reached its peak by February 4. Infections started to decline afterward and reached the bottom in about one month.[17] Panel B reports the daily death counts averaged across all cities which exhibit a similar pattern. Panel C displays average infections for each city throughout the sample period, where the darker colors denote cities with higher levels of infections and lighter colors denote cities with lower levels of infections. Significant spatial correlations presented in the map justify our approach of incorporating spatial dependence in the model.[18]

[PLACE FIGURE 1 HERE]

We obtain city-specific measures of population density and government efficiency from the *2019 Global Urban Competitiveness Yearbook*. The extent of city agglomeration is measured by the population density in our baseline estimation. We further take into consideration both city area size and population density in various robustness checks to reflect

[17] Manski and Molinari (2020) note that the infection rate might be substantially higher than reported based on data from Illinois state and New York state in the U.S. and Italy.

[18] We remove Wuhan, the epicenter of the COVID-19 outbreaks, in our regression sample to avoid issues related to extreme centrality and measurement errors. In the setting of SAR models with social interactions, the unit associated with an extremely high Bonacich (1987) measure may dominate in its own spatial effect on neighbors but is less subject to the feedback spatial effect (Liu and Lee, 2010). Moreover, Wuhan followed especially stringent lock down orders and received a vast amount of centrally deplored resources in fighting against the virus transmission. Those aspects are not accurately and consistently measured in our data. To avoid potential estimation bias, we incorporate Wuhan' s spatial effect on its neighbors when constructing the spatial weight matrices but remove Wuhan from the final regression sample when estimating the spatial effect in equilibrium.

agglomeration effects manifested through both the extensive margin and the intensive margin (Combes and Gobillon, 2015).[19] Government efficiency measure is based on comprehensive survey questions and reflects the city's management capacity to utilize limited resources to generate wealth. We also obtain city-specific measures of GDP, income per capita, employment, transportation infrastructure, and human capital from this yearbook to support a set of robustness checks. [20]

The third data source is the 2019 *Statistical Yearbook of China* from which we collect the number of hospital beds per 1,000 people as a proxy for city-specific medical resources in our baseline specification. As a robustness check, we also use the number of medical staff from the same data as an alternative proxy. Summary statistics are given in Table A1. Figure 2 plots the correlation between city population and the three key measures used in our empirical analysis: population density, government efficiency, and the amount of medical resources. Cities with a larger population size are associated with higher population density, higher city efficiency, and

[19] In the extensive literature assessing the benefits and costs of city agglomeration, employment is generally preferred to population in measuring the city scale as it better reflects the magnitude of local economic activities. In our context, population measure is more appropriate because our sample period covers the Chinese Spring Festival when majority of migrant workers travel back home to celebrate the festive season.

[20] The appendix of this paper provides detailed explanations on the construction of city-level indexes to measure various aspects of cities' competitiveness. One caveat is that the government efficiency measure based on information *before* COVID-19 may not reflect the true government efficiency *during* COVID-19. If such measurement error occurs randomly, we suffer from the standard attenuation bias. In such a scenario, we claim that the estimated impact of government efficiency on infection and death outcomes is understated. However, such measurement errors may not be random. A likely scenario is that cities short of effective management in combating the pandemic suddenly receive additional central government support/resources and experience an increase in their effectiveness in coping with COVID-19. This scenario again would lead to a downward bias in the magnitude of the estimated coefficients.

more abundant medical resources. Figure 3 reports the kernel density estimates for city characteristics.

[PLACE FIGURE 2 HERE]

[PLACE FIGURE 3 HERE]

The last dataset contains information on the intensity of travel between city pairs which is provided by Baidu (https://qianxi.baidu.com). This information allows us to construct two versions of the spatial weight matrix, one of which is used in our baseline specification and the other in robustness checks.[21] Although the dataset provides time variation in travel flows between city pairs, we do not explore this time variation in capturing the extent of cross-city contagion as timely travel flows are adversely affected by the infection and death outcomes. Instead, we collapse the pairwise inflow travel intensity for two weeks either before the sample starts (baseline) or at the beginning of the sample (robustness check) and use this cross-sectional variation to construct the spatial weight matrix. Compared to the classic spatial weight matrix computed based on either spatial contiguity or geographic distance, the travel information is more economically relevant.

5. RESULTS

5.1 Baseline estimates

Table 1 presents the results on the impact of city characteristics on COVID-19 infection and death outcomes. To allow the estimated coefficients to vary with different phases of the epidemic cycle, we conduct the model estimation separately for the pre-peak period and the post-peak period. Columns (1)-(4) report the estimation coefficients based on the pre-peak

[21] One caveat of this data is that only the shares of top 100 destinations are reported. However, this amounts to about 95% of the total travel intensity.

sample and Columns (5)-(8) report the estimation coefficients based on the post-peak sample. In Columns (1)-(2) and (5)-(6), we report results from the single equation 2SLS estimation for the infections and deaths equations. In Columns (3)-(4) and (7)-(8), we report results from the system 3SLS estimation, taking into consideration the correlation between the infections and deaths equations.

[PLACE TABLE 1 HERE]

A few patterns emerge. First, there exists a significant correlation between infections and deaths for the pre-peak period after partialling out city fixed effects, time fixed effects, and other control variables. Such a strong correlation is expected due to the simultaneity of infections and deaths. However, the correlation between infections and deaths in the post- peak period is small. It is possible that, during the post-peak period, public health measures and medical treatments are more standardized across cities in reducing social contacts and treating the infected. Hence, the time-lagged infections and city-specific controls that we include in the death equation explain a larger variation in the data for the post-peak period than the pre-peak period, leaving a small residual correlation in the errors.

Second, both the spatial and the temporal dynamic effects are strong and statistically significant. The significant spatial effect is consistent with prevalent cross-city transmissions. It highlights the importance of incorporating city-to-city spatial dependence in modeling infections. This effect is stronger in the pre-peak period than in the post-peak period, suggesting that necessary measures to prevent cross-city transmission in the early phase of the epidemic are crucial.[22] The significant impact of time-lagged infections is consistent with the time

[22] This finding questions the empirical assumptions imposed in Jia et al (2020) and Li and Ma (2020) that there are few cross-city transmissions among regions outside the epicenter of the early phase of the pandemic in China.

dynamics of the disease transmission. The lagged new infection cases are positively correlated with current new infections in both the pre-peak and the post-peak periods.

The main focus of our analysis is on the interaction terms involving time-lagged infections and city characteristics, i.e., the interactions of lagged infections with city population density and government efficiency. Not surprisingly, population density is significant in altering the time dynamics of new infection counts. Controlling for lagged infections, higher urban density leads to further increases in new infections. This is consistent with the intuition that urban density increases the extent of proximity when people interact in a community which in turn affects disease infection. Another crucial factor that significantly explains the extent to which previous infections lead to current infections is the measure of government efficiency. Evidence suggests that efficient government management reduces infections, holding the previous level of infections fixed. This finding highlights the important role of government in organizing resources and designing and implementing effective public health policies in fighting the pandemic.

It is also important to note that both urban density and government efficiency present different magnitudes for the impact of the pre-peak and the post-peak periods. In the early phase of the transmission, both urban density and government efficiency show a strong impact in altering the process of transmission. However, the impact of government efficiency is more muted in the post-peak period compared to the impact of population density. The evidence suggests that policy interventions at the early phase of the pandemic are more important in deterring the disease than in the latter phase of the epidemiological cycle.

The findings that the urban density and government efficiency present opposite impacts with similar magnitudes help to reconcile the findings in the literature on the small and insignificant impact of city size and population density (Li and Ma, 2022; Qiu et al. 2020). Given that there exists a high correlation between urban density and government efficiency, as

highlighted in Figure 2, failing to control for government efficiency may lead to a small and insignificant impact of urban density on infection and death outcomes. In other words, large cities did not experience widespread outbreaks in the early phase of the pandemic in China because their highly efficient government management mitigates the potential high transmission risk induced by high population density.

As to the determinants of death counts, we find that previous infections significantly contribute to the current death. In addition, the availability of medical resources reduces the number of deaths, holding previous infections fixed. The impact of medical resources is slightly stronger for the post-peak period than the pre-peak period, suggesting an improvement in the effectiveness of medical interventions over time.

[PLACE TABLE 2 HERE]

Table 2 reports the marginal effects of city characteristics on the number of infections before and after the peak. Since the spatial lagged dependent variable in the infection equation allows for the "global spillover" effect (a change in a regressor for one city can potentially affect the infections in all other cities), the slope coefficients in the model cannot be directly interpreted as the partial effects on the infections. To account for the spatial spillover effect, we calculate a direct effect and an indirect effect for each regressor. The direct effect measures the average impact on the number of infections of a city i arising from a change in a regressor in the same city, while the indirect effect measures the average impact on the number of infections in city i arising from a change in a regressor in all other cities $j \neq i$.

We calculate and report the marginal effects separately for the direct effects and the indirect effects in Table 2. Columns (1)-(4) show the marginals for the pre-peak estimates and Columns (5)-(8) report the marginals for the post-peak estimates. Patterns are similar to Table 1 but there exist varying degrees of the effect coming through either the direct channel or the indirect channel. For the pre-peak period, a larger impact is driven by the direct channel, but

the indirect channel is also quantitatively important. For the post-peak period, the majority of the impact is coming through the direct channel and the indirect channel is quantitatively small despite its significance. The strong indirect spatial channel reflects the importance of inter-city collaboration in curbing the virus transmission, especially in the early phase of the outbreak.

Controlling for lagged infections, the estimated marginal effects in Columns (3) and (4) demonstrate the extent to which population density and government efficiency affect the city-specific infection outcomes in a dynamic structure. Specifically, in the pre-peak period and conditional on lagged infections, a city with population density in the 75th percentile has 29% more infections through the direct channel and 20% more infections through the indirect channel, compared to a city with population density in the 25th percentile.[23] In the pre-peak period and conditional on lagged infections, a city with government efficiency in the 75th percentile has 27% fewer new infection cases through the direct channel and 18% fewer new infection cases through the indirect channel, compared to a city with government efficiency in the 25th percentile. [24] Evidence suggests that the impact of government efficiency is strong

[23] The city with population density measure at the 25th percentile is Liaoyuan in Jilin province, and the corresponding density index is 0.2346. The city with population density measure at the 75th percentile is Guiyang in Guizhou province, and the corresponding density index is 0.3464. Based on the estimated marginal effect of 2.6103 in Column (3) of Table 2, the marginal effect of density on the *level* of infection is mean(infection) X 2.6103. Therefore, the direct effect of increasing the density measure from the 25th percentile to the 75th percentile on the *percentage change* in infections is mean(infection) X 2.6103 X (0.3464-0.2346) / mean(infection) = 29%. The indirect effect of increasing the density measure from the 25th percentile to the 75th percentile is mean(infection) X 1.8079 X (0.3464-0.2346) / mean(infection) = 20%.

[24] The government efficiency index at the 25th percentile is 0.199, and at the 75th percentile is 0.282. Increasing the government efficiency index from the 25th percentile to the 75th percentile generates a direct effect of (-3.2126) X (0.282-0.199) = -27% in infections, and an indirect effect of (-2.2235) X (0.282-0.199) / mean(infection) = -18% in infections.

enough to almost mitigate all potential negative impacts of urban density. We also find that both effects become smaller in magnitude but quantitatively important for the post-peak period.

[PLACE TABLE 3 HERE]

In Table 3, we report the average effect throughout the full cycle. We report the estimated coefficients in Columns (1)-(4) and the marginal effects on infections in Columns (5)-(8). Taken together, we find that the urban density positively increases the current infections, and that government efficiency decreases the incidence of infections. The majority of the impact takes place through the direct channel, but the indirect channel is also quantitatively important and significant. We also find a similar impact of medical resources in reducing the number of deaths, conditional on previous infections.

5.2 Robustness checks

We embark on a collection of additional empirical exercises to check for robustness of our estimates to alternative spatial weight matrices, alternative specifications for the infection and death equations, including lagged spatial effect, an alternative proxy for medical resources, and death count dynamics, additional controls for efficiency, medical resources and economic development, alternative approaches to account for connectivity of the epicenter, additional controls for the role of the city area size as well as the role of other city characteristics.

5.2.1 Alternative spatial weight matrices

Table 4 reports the estimated coefficients for three alternative spatial weight matrices. The first spatial weight matrix is an alternative weight matrix based on the travel intensity averaged across the first two weeks at the beginning of the sample period. Two other spatial weight matrices are based on contiguity and geographic distance. For the contiguity-based spatial weight matrix, the element w_{ij} of W takes value 1 if cities i and j share the same border and 0 otherwise. As cities are not considered as neighbors to themselves, the diagonal elements w_{ii}

are set equal to 0 for $i = 1, 2, \ldots, n$. Then, we row-normalize all elements to obtain the spatial weight matrix, W. For the distance-based spatial weight matrix, we take the inverse distance as the element before row-normalizing the elements. Given the setup, the spatial lag of the dependent variable $WInfections_t$ captures a weighted average of infections in the neighboring cities and the i^{th} element of $WInfections_t$ is expressed as $\sum_{j=1}^{n} w_{ij} Infections_{jt}$, where $Infections_{jt}$ represents the number of new cases in city j at time t.

[PLACE TABLE 4 HERE]

The estimated coefficients are largely consistent across different spatial weight matrix specifications, with albeit small differences. The first noticeable difference is that the spatial effects are most pronounced when we use the inverse distance-based spatial weight matrix. This is largely driven by that the inverse distance-based spatial weight matrix is less sparse and allows for more, albeit heavily diluted, interactions between cities. The second noticeable difference is that the spatial effect is the smallest, but the impact of government efficiency is most pronounced when the spatial weight matrix is defined based on contiguity. This could be because contiguous cities are more likely to cooperate which minimizes spatial transmission and maximizes the effectiveness of local anti-corona virus measures.

5.2.2 Lagged spatial effect

Despite the justifications for the contemporaneous spatial effect in classic spatial dynamic panel data models, one might also be interested in a lagged spatial effect that incorporates not only equilibrium spatial patterns but also time dynamics associated with the spatial term. We present evidence of this in Columns (1) and (2) of Table 5. The estimated coefficients of the lagged spatial infection term are smaller because the lagged infections of neighboring cities are less correlated with the current infections of a target city, leaving more unexplained variations

in infections to be explained by lagged infections. However, we still obtain clear evidence on the impact of urban density and government efficiency.

[PLACE TABLE 5 HERE]

5.2.3 Alternative Proxy for Medical Resources

In Columns (3) and (4) of Table 5, we examine the robustness of the proxy for the abundance of medical resources. In the baseline regression, we use the number of hospital beds to proxy for medical resources. However, temporary medical facilities are built quickly during this period to treat and quarantine infected patients. To alleviate this concern, we experiment with using the number of medical staff, as opposed to the number of hospital beds, as a proxy for the availability of medical resources. Although medical staff are also mobile and can be dispatched to facilitate the treatment in other cities, the combined and consistent evidence on the number of hospital beds and the number of medical staff help alleviate potential concerns on whether those proxies are working as intended. Once again, the results are fairly robust to the measure of medical resources used.

5.2.4 Death count dynamics

In our baseline specification, we assume away any potential dynamics associated with the death outcomes. This assumption could be violated if previous death outcomes affect the current availability of medical resources, the current effectiveness of medical treatment, and also the mental status of current patients. Therefore, we alleviate this restriction by allowing for the time series dynamics for the death outcomes. We present the findings in Columns (5) and (6) of Table 5. We find that lagged death outcomes are positively correlated with current death counts. This effect dilutes some of the impact previously absorbed in the coefficient associated with lagged infections. The magnitude of the impact of medical resources also becomes smaller. However,

the key evidence on the impact of urban density and government efficiency on infections remains largely unchanged.

5.2.5 Impact of Efficiency on Deaths

In Columns (1) and (2) of Table 6, we experiment with adding government efficiency interactions to the death equation. The underlying rationale is that the ability of the local government in managing medical resources may directly affect how efficiently the infected receive medical treatment and how likely they subsequently recover from the disease. We find that government efficiency does play a significant role in reducing death tolls while maintaining its significant impact on reducing infections.

[PLACE TABLE 6 HERE]

5.2.6 Impact of Hospital Beds on Infections

In our baseline specification, we consider that medical resources mainly work through impacting the death outcomes. However, better and timely treatments of the infected may reduce future infections. In Columns (3) and (4) of Table 6, we add the interaction of lagged infections with the number of hospital beds to the infection equation, we observe a significant role of medical resources in reducing infection outcomes. Hospital beds remain important in reducing death tolls at the same time.

5.2.7 Role of GDP and Income per Capita

The level of economic development could matter in the dynamics of the infection and death outcomes because residents in more developed cities have more resources to cope with adverse shocks. In Columns (5) and (6), we further control for the interaction of lagged infections with city-specific GDP and the interaction of lagged infections with city-specific income per capita. We observe a significant positive impact of GDP on infections. This could be because measures of economic development are highly correlated with the population density and, hence, capture

a part of the variations in population density. The income per capita plays a significant role in reducing death tolls, while the role of medical resources is muted in the death equation, which could be driven by the high correlation between the number of hospital beds and measures of economic development. In Columns (7) and (8), we adopt a specification that includes the full set of controls presented in Columns (1)-(6), the findings remain robust.

5.2.8 Connectivity to the Epicenter

One concern on the potential misspecification of our baseline model is that the initial values for the dynamics of infections are not sufficient to capture the impact of a city's connectivity to the epicenter of the pandemic. As the city's infection and death outcomes are significantly affected by its population inflows from the city experiencing the initial outbreak, failing to properly account for the connectivity to the epicenter could result in biased estimates of our explanatory variables.

To address this concern, we adopt two approaches. First, we remove the first week of the sample in which cities may continue receiving a significant share of the population inflows from the epicenter. Such continuous shocks may change the dynamics that we modeled in the baseline specification because the dynamics of the current infections driven by the lagged infections of own cities and nearby cities could vary at the beginning versus at the later phase of the transmission. Focusing on the period of the sample in which the lockdown of the epicenter has already taken effect helps to mitigate such concerns. We report the corresponding results in Columns (1) and (2) of Table 7.

[PLACE TABLE 7 HERE]

Second, to account for the possibility of breakage to the lock-down policy or a prolonged incubation period of Wuhan infected travelers, we directly control for daily population inflows from Wuhan provided by the Baidu migration database. We report the corresponding estimates

in Columns (3)-(6) of Table 7. In Columns (3) and (4), we report findings after adding this additional control to our baseline specification. In Columns (5) and (6), we report these findings after adding this additional control to the specification presented in Columns (7) and (8) of Table 6. Note that in both cases, the sample size becomes smaller than that for the baseline specification because the information on daily population inflows from Wuhan is only available between January 20, 2020, and March 13, 2020. Despite the smaller sample size, the main findings on the role of city population density and government efficiency remain robust.

5.2.9 Extensive Margin of City Size

To preserve the power of identification, we choose to only focus on the intensive margin of city size and the role of government efficiency in our baseline model. As a robustness check, we control for the role of the city area size to understand the extensive margin of the city effect. We report the estimated coefficients in Columns (1) and (2) of Table 8. Not surprisingly, larger cities have more infections conditional on the population density and government efficiency. More importantly, the additional control of the interactive effect of the city area size does not dramatically change the magnitudes of the impacts of population density and government efficiency.

[PLACE TABLE 8 HERE]

5.2.10 Role of Employment, Transport Infrastructure, and Human Capital

One concern with the interpretation of the impact of government efficiency is that this proxy might be correlated with other city-level characteristics, and it could be mainly those other characteristics that drive the change in the prevalence of infections. To alleviate these concerns, we further control for three key city-specific features-the employment size, the extent of the transportation infrastructure build-up, and the level of city-specific human capital - in a different set of robustness checks. Results are reported in Columns (3)-(8) of Table 8 which

show that our baseline estimates of city government efficiency are about the same magnitudes despite additional controls.

6. CONCLUSION

Urban density brings in significant benefits manifested through improved access to goods and services, enhanced productivity, and reduced travel costs. It also comes with various costs in the form of congestion, concentrated crimes, pollution, as well as propagation of contagious diseases (Duranton and Puga, 2020). We focus on highlighting the cost of cities in the context of the COVID-19 pandemic and potential counteracting forces that may mitigate the cost. By fitting a simultaneous spatial dynamic panel data model with information on early COVID-19 transmissions in China, we show that population density plays a significant role in contributing to the wide prevalence of infected cases and resulting deaths across Chinese cities. Despite the significant cost of urban density measured in terms of infections and deaths, we also find that effective city government management mitigates the potential cost through possible effective implementations of public health measures. In addition, conditional on the number of lagged infections, medical resources that are more abundant in larger cities effectively reduce the number of deaths in those cities.

We acknowledge that this aspect of the urban cost that we highlight in this paper operates at a very different intertemporal scale than that related to most considerations on urban benefits, so they are not directly comparable. However, with significant uncertainty associated with how long the current pandemic may last and the possibility of future re-current outbreaks, it is essential to factor in the public health costs that density entails to better understand the trade-off between the cost and benefit of cities.[25] Moreover, the evidence on the importance of the

[25]For instance, Kissler et al. (2020) project that recurrent wintertime outbreaks of the virus are likely occur and a resurgence in contagion could be possible as late as 2024.

city government efficiency in a pandemic provides broad implications for the potential role of government practices in mitigating widely documented costs of big cities, such as pollution and congestion.

As a final note, our analysis does not speak directly to the policy debate on whether to adopt stringent controls to clear out the virus or mitigating measures to flatten the curve of virus transmissions. However, in the context of early COVID-19 transmissions in China in which knowledge about the COVID-19 virus was sparse and no effective treatment or vaccination for the disease was available, it was sensible to adopt a zero COVID policy with the aim to curb disease transmissions as effectively as possible. This context provides a credible opportunity to study the role of government efficiency as it ensures that our government efficiency measure accurately reflects the effectiveness of local government in achieving a clearly specified and nationwide homogenous objective.

ACKNOWLEDGEMENTS

We would like to thank the Co-Editor, Professor Edward Coulson, and two anonymous referees for their insightful and constructive comments, which led to significant improvements in the paper. We thank conference participants at the 2021 European Meeting of the Urban Economics Association for their helpful comments. Jing Li gratefully acknowledges the financial support from Singapore Management University under the Lee Kong Chian Fellowship. Remaining errors are our own.

REFERENCES

Acemoglu, D., C. Garcia-Jimeno, & J. A. Robinson (2015). State Capacity and Economic Development: A Network Approach. *American Economic Review 105*, 2364–2409.

Acemoglu, D., J. Moscona, & J. A. Robinson (2016). State Capacity and American Technology: Evidence from the Nineteenth Century. *American Economic Review 106*, 61–67.

Adda, J. (2016). Economic Activity and the Spread of Viral Diseases: Evidence from High Frequency Data. *Quarterly Journal of Economics 131*, 891–941.

Almagro, M. & A. Orane-Hutchinson (2020). The Determinants of the Differential Exposure to COVID-19 in New York city and Their Evolution Over Time. *Journal of Urban Economics* (Forthcoming).

Antras, P., S. J. Redding, & E. Rossi-Hansberg (2020). Globalization and Pandemics. *NBER Working Paper Series*.

Arellano, M. & O. Bover (1995). Another Look at the Instrumental Variable Estimation of Error-Components Models. *Journal of Econometrics 68*, 29–51.

Argente, D., Hsieh, C. T., & Lee, M. (2022). the Cost of Privacy: Welfare Effects of the Disclosure of Covid-19 Cases. *Review of Economics and Statistics*, *104*(1), 176–186.

Ashraf, B. N., E. L. Glaeser, & G. A. M. Ponzetto (2016). Infrastructure, Incentives, and Institutions. *American Economic Review: Papers and Proceedings 106*, 77–82.

Baltagi, B. H. (2021). *Econometric Analysis of Panel Data*, 6th edition. Switzerland: Springer.

Bisin, A. & A. Moro (2020). Learning Epidemiology by Doing: The Empirical Implications of a Spatial Sir Model with Behavioral Responses. *SSRN Electronic Journal*.

Bottasso, A., Cerruti, G., & Conti, M. (2022). Institutions matter: The impact of the covid-19 pandemic on the political trust of young Europeans. *Journal of Regional Science*, *September 2021*.

Brzezinski, A., G. Deiana, V. Kecht, & D. V. Dijcke (2020). The COVID-19 Pandemic: Government vs. Community Action Across the United States. *Covid Economics 7*, 115–156.

Cameron, A. C. & P. K. Trivedi (2005). *Microeconometrics: Methods and Applications*. Cambridge: Cambridge University Press.

Carozzi, F., S. Roth, & S. Provenzano (2020). Urban Density and COVID-19. *IZA Discussion Paper*.

Chinazzi, M., J. T. Davis, M. Ajelli, C. Gioannini, M. Litvinova, S. Merler, A. P. Y. Piontti, L. Rossi, K. Sun, C. Viboud, X. Xiong, H. Yu, M. E. Halloran, I. M. Longini, & A. Vespignani,

(2020). The Effect of Travel Restrictions on the Spread of the 2019 Novel Coronavirus (2019-nCoV) Outbreak. *Science*, *368*, 395–400.

Combes, P. P. & L. Gobillon (2015). The Empirics of Agglomeration Economies. *Handbook of Regional and Urban Economics 5*, 247–348.

Crow, D. & H. Kuchler (2020). US Coronavirus Surge: 'It's a Failure of National Leader- ship'. *Financial Times*, July 18.

Cunat, A. & R. Zymek (2020). The (Structural) Gravity of Epidemics. *CESifo Working Paper Series*.

Cutler, D. & G. Miller (2005). The Role of Public Health Improvements in Health Advances: The Twentieth-Century United States. *Demography 42*, 1–22.

Dave, D., A. Friedson, K. Matsuzawa, J. J. Sabia, & S. Safford (2020). Were Urban Cowboys Enough to Control COVID-19? Local Shelter-in-place Orders and Coronavirus Case Growth. *Journal of Urban Economics* (Forthcoming).

Desmet, K. & R. Wacziarg (2020). Understanding Spatial Variation in COVID-19 across the United States. *NBER Working Paper Series*.

Duranton, G. & D. Puga (2020). The Economics of Urban Density. *Journal of Economic Perspectives 34*, 3–26.

Fang, H., L. Wang, & Y. Yang (2020). Human Mobility Restrictions and the Spread of the Novel Coronavirus (2019-nCoV) in China. *SSRN Electronic Journal*.

Glaeser, E. L. (2011). *Triumph of the City: How Our Greatest Invention Makes Us Richer, Smarter, Greener, Healthier, and Happier*. London: MacMillan.

Glaeser, E. L., C. S. Gorback, & S. J. Redding (2020). How Much does COVID-19 Increase with Mobility? Evidence from New York and Four Other U.S. Cities. *NBER Working Paper Series*.

Greenstone, M. & V. Nigam (2020). Does Social Distancing Matter? *University of Chicago, Becker Friedman Institute for Economics Working Paper*.

Hayakawa, K. (2009). First Difference or Forward Orthogonal Deviation - Which Transfor- mation should be used in Dynamic Panel Data Models?: A Simulation Study. *Economics Bulletin 29*, 2008–2017.

Jia, J.S. , Lu, X. , Yuan, Y. , Xu, G. , Jia, J. , Christakis, N.A. , 2020. Population flows drives spatio-temporal distribution of Covid-19 in China. *Nature*.

Kelejian, H. H. & I. R. Prucha (1998). A Generalized Spatial Two-Stage Least Squares Procedure for Estimating a Spatial Autoregressive Model with Autoregressive Disturbances. *Journal of Real Estate Finance and Economics 17*, 99–121.

Kissler, S. M., C. Tedijanto, E. Goldstein, Y. H. Grad, & M. Lipsitch (2020). Projecting the Transmission Dynamics of SARS-CoV-2 through the Postpandemic Period. *Science 368*, 860–868.

Krugman, Paul. 2020. "3 Rules for the Trump Pandemic." New York Times. March 19. https://www.nytimes.com/2020/03/19/opinion/trump-coronavirus.html

Kuchler, T., D. Russel, & J. Stroebel (2021). The Geographic Spread of COVID-19 Cor- relates with the Structure of Social Networks as Measured by Facebook. *Journal of Urban Economics* (Forthcoming).

Lee, K. O., & Lee, H. (2021). Public responses to COVID-19 case disclosure and their spatial implications. *Journal of Regional Science*, *March*.

Lee, L. & J. Yu (2014). Efficient GMM Estimation of Spatial Dynamic Panel Data Models with Fixed Effects. *Journal of Econometrics 180*, 174–197.

Leonhardt, D. (2020). The Unique U.S. Failure to Control the Virus. *New York Times*, August 06.

Li, B. & L. Ma (2020). Migration, Transportation Infrastructure, and the Spatial Trans- mission of COVID-19 in China. *Journal of Urban Economics* (Forthcoming).

Li, J. (2014). The Influence of State Policy and Proximity to Medical Services on Health Outcomes. *Journal of Urban Economics 80*, 97–109.

Maloney, W. & T. Taskin (2020). *Determinants of Social Distancing and Economic Activity during COVID-19: A Global View*. The World Bank.

Mangrum, D. & P. Niekamp (2020). College Student Travel Contributed to Local COVID- 19 Spread. *Journal of Urban Economics* (Forthcoming).

Manski, C. F. & F. Molinari (2020). Estimating the COVID-19 Infection Rate: Anatomy of an Inference Problem. *Journal of Econometrics* (Forthcoming).

Narita, Y., & Sudo, A. (2021). Course of Democracy: Evidence from 2020. SSRN Electronic Journal.

Neyman, J. & E. L. Scott (1948). Consistent Estimates Based on Partially Consistent Observations. *Econometrica 16*, 1–32.

Nickell, S. (1981). Biases in Dynamic Models with Fixed Effects. *Econometrica 49*, 1417–1426.

Phillips, R. F. (2019). A Comparison of First-Difference and Forward Orthogonal Deviations GMM. *arXiv:1907.12880*.

Qiu, Y., X. Chen, & W. Shi (2020). Impacts of Social and Economic Factors on the Transmission of Coronavirus Disease 2019 (COVID-19) in China. *Journal of Population Economics 33*, 1127–1172.

Rodríguez-Pose, A., & Burlina, C. (2021). Institutions and the uneven geography of the first wave of the COVID-19 pandemic. *Journal of Regional Science*, *61*(4), 728–752.

Troesken, W. (2002). The Limits of Jim Crow: Race and the Provision of Water and Sewerage Services in American Cities, 1880-1925. *Journal of Economic History 62*, 734–772.

Vespignani, A. (2020). The Effect of Travel Restrictions on the Spread of the 2019 Novel Coronavirus (2019-nCoV) Outbreak. *Science 368*, 395–400.

Wheaton, W. C. & A. K. Thompson (2020a). The Geography of COVID-19 Growth in the US: Counties and Metropolitan Areas. *SSRN Electronic Journal*.

Wheaton, W. C. & A. K. Thompson (2020b). Doubts about Density: COVID-19 across Cities and Towns. *SSRN Electronic Journal*.

Xie, L., H. Yang, X. Zheng, Y. Wu, X. Lin, & Z. Shen (2021). Medical Resources and Coronavirus Disease (COVID-19) Mortality Rate: Evidence and Implications from Hubei Province in China. *PLoS ONE 16*, 1–13.

Yang, K. & L. Lee (2019). Identification and Estimation of Spatial Dynamic Panel Simultaneous Equations Models. *Regional Science and Urban Economics 76*, 32–46.

TABLE 1: The Impact of City Characteristics on Number of Infections and Deaths Based on Travel Intensity Weight Before and After the Peak

	Before the Peak (2020.1.20-2020.2.4)				After the Peak (2020.2.5-2020.3.31)			
	Single		System		Single		System	
	Infections	**Deaths**	**Infections**	**Deaths**	**Infections**	**Deaths**	**Infections**	**Deaths**
	(1)	(2)	(3)	(4)	(5)	(6)	(7)	(8)
W×Infections	0.4174***		0.4234***		0.0802***		0.0871***	
	(18.9765)		(19.7581)		(43.7078)		(47.3456)	
L. Infections	0.5292***	0.0062***	0.5092***	0.0033***	0.3608***	0.0121***	0.2616***	0.0127***
	(8.0336)	(18.3189)	(7.8380)	(9.1230)	(8.4640)	(41.7331)	(6.1400)	(40.8835)
L.Infections×Density	2.5753***		2.5452***		0.7917***		1.0337***	
	(12.2561)		(12.3486)		(8.5600)		(11.1678)	
L.Infections×Efficiency	-3.2495***		-3.1312***		-0.8797***		-0.8876***	
	(-11.7461)		(-11.6172)		(-7.9302)		(-7.9802)	
L.Infections×Num of Beds		-0.0072***		-0.0056***		-0.0063***		-0.0112***
		(-5.3325)		(-3.9392)		(-3.9435)		(-5.4312)
Constant	-3.0158***	-0.0245**	1.7344***	-0.0277**	0.0239	-0.0226*	2.0211***	-0.0216*
	(-5.6818)	(-2.2569)	(3.4451)	(-2.5328)	(0.0907)	(-1.7280)	(7.5729)	(-1.6551)
R-Squared	0.3570	0.0732	0.3472	0.0569	0.5237	0.1233	0.4901	0.1228
ρ	0		-0.3677		0		-0.0831	
Observations	4,950		4,950		18,150		18,150	

*Notes: Columns (1)-(4) are coefficients for single equations and system of equations before the peak. Columns (5)-(8) are coefficients for single equations and system of equations after the peak. We control for city and time fixed effects. ρ represents cross-equation correlations between $u_{1,it}$ and $u_{2,it}$. *p < .10, **p < .05, ***p < .01. t-stats are reported in parentheses.*

TABLE 2: Marginal Effects of City Characteristics on Number of Infections Based on Travel Intensity Weight Before and After the Peak

	Before the Peak (2020.1.20-2020.2.4)				**After the Peak (2020.2.5-2020.3.31)**			
	Single		System		Single		System	
	Direct	**Indirect**	**Direct**	**Indirect**	**Direct**	**Indirect**	**Direct**	**Indirect**
	(1)	(2)	(3)	(4)	(5)	(6)	(7)	(8)
L. Infections	0.5446***	0.3645***	0.5237***	0.3603***	0.3602***	0.0311***	0.2625***	0.0247***
	(8.6505)	(8.8059)	(8.0349)	(8.2270)	(8.7681)	(9.3360)	(5.9963)	(6.2105)
L.Infections×Density	2.6387***	1.7781***	2.6103***	1.8079***	0.7939***	0.0687***	1.0343***	0.0976***
	(12.6531)	(7.2442)	(12.4702)	(7.3333)	(8.655)	(7.8987)	(11.1208)	(10.0654)
L.Infections×Efficiency	-3.3320***	-2.2433***	-3.2126***	-2.2235***	-0.8791***	-0.0760***	-0.8888***	-0.0838***
	(-12.1584)	(-7.4722)	(-11.2382)	(-7.2898)	(-8.1435)	(-7.8965)	(-7.7584)	(-7.6126)
R-Squared	0.3570	0.0732	0.3472	0.0569	0.5237	0.1233	0.4901	0.1228
ρ	0		-0.3677		0		-0.0831	
Observations	4,950		4,950		18,150		18,150	

Notes: Columns (1)-(2) are marginal effects for the regression of column (1) in Table 1. Columns (3)-(4) are marginal effects for the regression of column (3) in Table 1. Columns (5)-(6) are marginal effects for the regression of column (5) in Table 1. Columns (7)-(8) are marginal effects for the regression of column (7) in Table 1. We control for city and time fixed effects. ρ represents cross-equation correlations between $u_{1,it}$ and $u_{2,it}$. $*p < .10$, $**p < .05$, $***p < .01$. t-stats are reported in parentheses.

TABLE 3: The Impact of City Characteristics on Number of Infections and Deaths Based on Travel Intensity Weight

	Coefficients				**Marginal Effects on Infections**			
	Single		System		Single		System	
	Infections	**Deaths**	**Infections**	**Deaths**	**Infections**	**Deaths**	**Infections**	**Deaths**
	(1)	(2)	(3)	(4)	(5)	(6)	(7)	(8)
W×Infections	0.0735***		0.0830***					
	(36.8593)		(41.6368)					
L. Infections	0.5755***	0.0104***	0.5036***	0.0099***	0.5752***	0.0452***	0.5049***	0.0452***
	(20.0945)	(45.7864)	(17.5986)	(41.4890)	(20.7518)	(21.0728)	(17.4525)	(18.1681)
L.Infections×Density	1.0606***		1.2511***		1.0611***	0.0834***	1.2514***	0.1122***
	(14.6655)		(17.2970)		(14.6376)	(12.063)	(17.4876)	(14.3166)
L.Infections×Efficiency	-1.5048***		-1.5672***		-1.5015***	-0.1180***	-1.5721***	-0.1409***
	(-16.3532)		(-16.9929)		(-16.4579)	(0.0834)	(-17.0438)	(-14.833)
L.Infections×Num of Beds		-0.0077***		-0.0095***				
		(-6.9541)		(-7.4539)				
Constant	0.0259	-0.0195	-0.0904	-0.0206				
	(0.0885)	(-1.5395)	(-0.3073)	(-1.6315)				
R-Squared	0.5670	0.1101	0.5401	0.1094	0.5670		0.5401	
ρ	0		-0.1006		0		-0.1006	
Observations	23100		23100		23100		23100	

*Notes: Columns (1)-(2) are coefficients for single equations of Infections and Deaths. Columns (3)-(4) are coefficients for system of equations. Columns (5)-(6) are marginal effects for regression in column (1). Columns (7)-(8) are marginal effects for regression in column (3). We control for city and time fixed effects. ρ represents cross-equation correlations between $u_{1,it}$ and $u_{2,it}$. *p < .10, **p < .05, ***p < .01. t-stats are reported in parentheses.*

TABLE 4: The Impact of City Characteristics on Number of Infections and Deaths Based on Different Weight Matrices

	Robust Travel Intensity		Contiguity		Distance	
	Infections	**Deaths**	**Infections**	**Deaths**	**Infections**	**Deaths**
	(1)	(2)	(3)	(4)	(5)	(6)
W×Infections	0.0758***		0.0523***		0.3701***	
	(39.0743)		(23.0210)		(23.2505)	
L. Infections	0.5245***	0.0099***	0.7456***	0.0096***	0.7621***	0.0098***
	(18.6576)	(41.5009)	(28.5546)	(40.4889)	(29.1179)	(41.1026)
L.Infections×Density	1.1966***		1.1047***		0.8874***	
	(16.8515)		(14.8648)		(12.4966)	
L.Infections×Efficiency	-1.5466***		-2.0271***		-1.6779***	
	(-17.1080)		(-20.5270)		(-17.9473)	
L.Infections×Num of Beds		-0.0094***		-0.0081***		-0.0083***
		(-7.3733)		(-6.3016)		(-6.5121)
Constant	-0.1031	-0.0206	-0.2318	-0.0205	1.1160***	-0.0204
	(-0.3576)	(-1.6290)	(-0.8368)	(-1.6227)	(3.9128)	(-1.6140)
R-Squared	0.5619	0.1095	0.6111	0.1094	0.6066	0.1096
ρ	-0.0935		-0.0130		0.0061	
Observations	23100		23100		23100	

Notes: Columns (1)-(2) are coefficients for system of equations based on an alternative travel intensity weighted spatial weight matrix. Columns (3)-(4) are coefficients for system of equations based on contiguity spatial weight matrix. Columns (5)-(6) are coefficients for system of equations based on distance weighted spatial weight matrix. We control for city and time fixed effects. ρ represents cross-equation correlations between $u_{1,it}$ and $u_{2,it}$. $*p < .10$, $**p < .05$, $***p < .01$. t-stats are reported in parentheses.

TABLE 5：Robustness to Death Count Dynamics, Lagged Spatial Effect, and an Alternative Proxy for Medical Resources

	Infections	Deaths	Infections	Deaths	Infections	Deaths
	(1)	(2)	(3)	(4)	(5)	(6)
W×Infections			0.0823***		0.0723***	
			(41.2954)		(38.4634)	
L.W×Infections	0.0129***					
	(16.1651)					
L. Infections	0.8230***	0.0098***	0.4934***	0.0092***	0.5532***	0.0057***
	(30.5109)	(41.3482)	(17.2866)	(46.2396)	(19.6749)	(25.7509)
L.Infections×Density	0.3575***		1.2682***		1.1091***	
	(5.2039)		(17.5769)		(15.5948)	
L.Infections×Efficiency	-0.8747***		-1.5397***		-1.4635***	
	(-9.6423)		(-16.7419)		(-16.0537)	
L.Infections×Num of Beds		-0.0008***				-0.0005***
		(-6.4002)				(-4.5222)
L.Infections×Num of Staff				-0.0024***		
				(-8.5619)		
L.Deaths						0.4729***
						(78.3054)
Constant	-0.2331	-0.0203	-0.0901	-0.0204	-0.1142	-0.0105
	(-0.8037)	(-1.6045)	(-0.3069)	(-1.6141)	(-0.3933)	(-0.9238)
R-Squared	0.5750	0.1097	0.5422	0.1096	0.5699	0.2769
ρ	0.0393		-0.102		-0.0330	
Observations	23100		23100		23100	

*Notes: Columns (1)-(2) consider the temporal lag of spatial dependence. Columns (3)-(4) replace number of beds with number of medical staff. Columns (5)-(6) consider the dynamics of death equation. All regressions control for city and time fixed effects. ρ represents cross-equation correlations between u1,it and u2,it. *p < .10, **p < .05, ***p < .01. t-stats are reported in parentheses.*

TABLE 6：Robustness to Controlling for Efficiency, Num of Beds, and Economic Development

	Infections	**Deaths**	**Infections**	**Deaths**	**Infections**	**Deaths**	**Infections**	**Deaths**
	(1)	(2)	(3)	(4)	(5)	(6)	(7)	(8)
W×Infections	0.0829***		0.0832***		0.0792***		0.0788***	
	(41.5671)		(41.8605)		(41.0189)		(41.2000)	
L. Infections	0.4985***	0.0158***	0.1181***	0.0098***	0.7068***	0.0167***	0.5031***	0.0173***
	(17.4144)	(17.5595)	(2.5793)	(41.1962)	(12.5809)	(16.4577)	(8.7365)	(16.6345)
L.Infections×Density	1.2348***		2.2501***		0.7207***		1.2531***	
	(17.0645)		(19.1693)		(4.5852)		(7.8109)	
L.Infections×Efficiency	-1.5177***	-0.0297***	-1.0375***		-1.7952***		-1.7189***	-0.0126*
	(-16.4064)	(-6.8527)	(-9.9234)		(-8.7106)		(-8.3851)	(-1.8516)
L.Infections×Num of Beds		-0.0048***	-0.6100***	-0.0090***		0.0003	-0.9749***	0.0020
		(-3.3469)	(-10.7525)	(-7.0073)		(0.0995)	(-15.1083)	(0.7362)
L.Infections×GDP					0.5769***	-0.0088	1.7889***	-0.0108*
					(3.9939)	(-1.6141)	(10.9052)	(-1.9366)
L.Infections×Income					-0.2905	-0.0293***	-0.6924***	-0.0191**
					(-1.5493)	(-4.8026)	(-3.6814)	(-2.4283)
Constant	-0.0888	-0.0215*	-0.1107	-0.0206	-0.0950	-0.0215*	-0.1221	-0.0216*
	(-0.3018)	(-1.7014)	(-0.3770)	(-1.6261)	(-0.3253)	(-1.7047)	(-0.4210)	(-1.7119)
R-Squared	0.5405	0.1118	0.5423	0.1095	0.5517	0.1115	0.5579	0.1118
ρ	-0.0986		-0.101		-0.0895		-0.0898	
Observations	23100		23100		23100		23100	

*Notes: Columns (1)-(2) control for government efficiency in the death equation. Columns (3)-(4) control for number of hospital beds in the infection equation. Columns (5)-(6) control for GDP and disposable income per capita in both equations. Columns (7)-(8) include all controls of models in Columns (1)-(6). All regressions control for city and time fixed effects. ρ represents cross-equation correlations between $u_{1,it}$ and $u_{2,it}$. *p < .10, **p < .05, ***p < .01. t-stats are reported in parentheses.*

TABLE 7：Robustness to Controlling for Connectivity to the Epicenter

	Infections	**Deaths**	**Infections**	**Deaths**	**Infections**	**Deaths**
	(1)	(2)	(3)	(4)	(5)	(6)
W×Infections	0.0863***		0.0826***		0.0782***	
	(42.2416)		(36.8442)		(36.2441)	
L. Infections	0.4659***	0.0104***	0.4875***	0.0094***	0.4996***	0.0181***
	(14.8972)	(41.1718)	(15.0000)	(34.5004)	(7.5718)	(15.1506)
L.Infections×Density	1.3055***		1.2747***		1.2404***	
	(16.8953)		(15.5275)		(6.7038)	
L.Infections×Efficiency	-1.6120***		-1.5317***		-1.7222***	-0.0200**
	(-16.6908)		(-14.3993)		(-7.2907)	(-2.5571)
L.Infections×Num of Beds		-0.0010***		-0.0009***	-0.0987***	0.0002
		(-7.1893)		(-5.6532)	(-12.8525)	(0.6009)
L.Infections×GDP					1.8092***	-0.0054
					(9.5711)	(-0.8314)
L.Infections×Income					-0.6637***	-0.0206**
					(-3.0451)	(-2.2755)
Inflow from Wuhan			0.9254***		0.8899***	
			(4.2128)		(4.0923)	
Constant	1.5651***	-0.0228*	-0.0728	-0.0208	-0.1074	-0.0219
	(5.1878)	(-1.7458)	(-0.2144)	(-1.4314)	(-0.3213)	(-1.5082)
R-Squared	0.5439	0.1042	0.5403	0.1094	0.5586	0.1119
ρ	-0.133		-0.136		-0.122	
Observations	19800		17160		17160	

*Notes: Columns (1)-(2) drop observations of the first week. Columns (3)-(4) control for daily inflow from Wuhan based on the model in Columns (1)-(2). Columns (5)-(6) include additional controls of GDP and disposable income per capita in both equations while controlling for daily outflow from Wuhan. All regressions control for city and time fixed effects. ρ represents cross-equation correlations between u_1,it and u_2,it. *p < .10, **p < .05, ***p < .01. t-stats are reported in parentheses.*

TABLE 8：Robustness to Controlling for Employment, Intra-city Mobility and Education

	Infections	**Deaths**	**Infections**	**Deaths**	**Infections**	**Deaths**	**Infections**	**Deaths**
	(1)	(2)	(3)	(4)	(5)	(6)	(7)	(8)
W×Infections	0.0810***		0.0771***		0.0776***		0.0770***	
	(41.9124)		(42.3074)		(42.6670)		(42.7344)	
L.Infections	0.2404*	0.0171***	0.7028***	0.0170***	0.6948***	0.0171***	0.8158***	0.0171***
	(1.9264)	(16.4182)	(5.5734)	(16.3787)	(5.4951)	(16.4450)	(6.3227)	(16.4367)
L.Infections×Density	1.4612***		0.6607***		0.6991***		0.5922***	
	(7.9925)		(3.5330)		(3.7080)		(3.1326)	
L.Infections×Efficiency	-1.5978***	-0.0141**	-1.5671***	-0.0144**	-1.5045***	-0.0157**	-1.6954***	-0.0156**
	(-7.3795)	(-2.0698)	(-7.3495)	(-2.1153)	(-6.9284)	(-2.3144)	(-7.6350)	(-2.3048)
L.Infections×Num of Beds	-0.9968***	0.0027	-0.9312***	0.0027	-0.9135***	0.0027	-1.0066***	0.0027
	(-15.2443)	(0.9994)	(-14.4216)	(0.9983)	(-14.1476)	(0.9773)	(-14.3687)	(0.9766)
L.Infections×GDP	1.4754***	-0.0116**	0.9506***	-0.0119**	0.9098***	-0.0114**	1.4363***	-0.0114**
	(6.7793)	(-2.0876)	(4.3613)	(-2.1265)	(3.6429)	(-2.0507)	(5.0348)	(-2.0457)
L.Infections×Income	-0.3731	-0.0163**	-1.0675***	-0.0156**	-1.1037***	-0.0149*	-1.4670***	-0.0150*
	(-1.6189)	(-2.0755)	(-4.6159)	(-1.9907)	(-4.7060)	(-1.9002)	(-5.7954)	(-1.9071)
L.Infections×Size	1.1704**		-0.7490		-0.8091		-1.1563**	
	(2.3446)		(-1.4808)		(-1.5361)		(-2.1736)	
L.Infections×Employment			1.3158***		1.3056***		1.3414***	
			(14.9440)		(14.4157)		(14.7979)	
L.Infections×Infrastructure					0.0126		-0.2516	
					(0.0885)		(-1.5948)	
L.Infections×Higher Education							0.3362***	
							(3.6747)	
Constant	-0.1122	-0.0215*	-0.1502	-0.0215*	-0.1472	-0.0215*	-0.1417	-0.0215*
	(-0.3851)	(-1.7051)	(-0.5232)	(-1.7052)	(-0.5121)	(-1.7058)	(-0.4936)	(-1.7058)
R-Squared	0.5514	0.1119	0.5677	0.1119	0.5664	0.1119	0.5682	0.1119
ρ	-0.0940		-0.0885		-0.0898		-0.0887	
Observations	23100		23100		23100		23100	

*Notes: Columns (1)-(2) control for city size in the infection equation. Columns (3)-(4) include additional control variable for the total employment to the previous model in Columns (1)-(2). Columns (5)-(6) include additional control variable for the intra-city mobility to the previous model in Columns (3)-(4). Columns (7)-(8) include additional control variable for higher education to the previous model in Columns (5)-(6). All regressions control for city and time fixed effects. ρ represents cross-equation correlations between $u_{1,it}$ and $u_{2,it}$. *p < .10, **p < .05, ***p < .01. t-stats are reported in parentheses.*

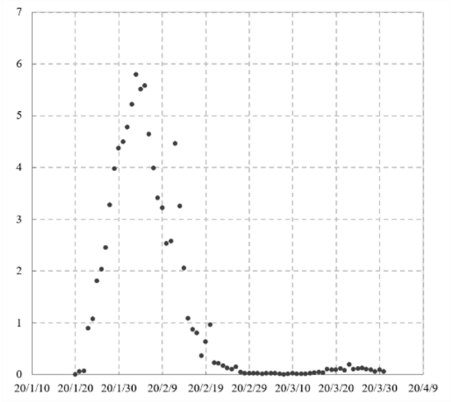

A. Daily Infections Averaged across All Cities

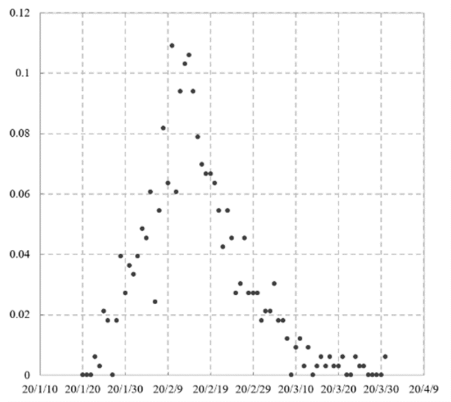

B. Daily Deaths Averaged across All Cities

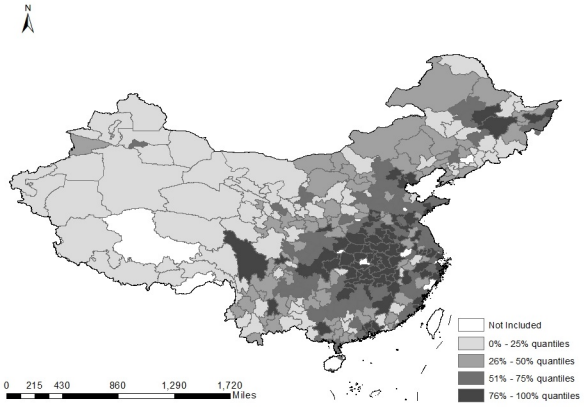

C. City Infections Averaged over All Time Periods

FIGURE 1: Infections and Deaths

Note: This figure reports the temporal and spatial patterns of the disease transmission. Panel A shows the daily new infection cases averaged across all 330 cities. Panel B reports the daily death counts averaged across all 330 cities. Panel C displays average infections for each city throughout the sample period, where the darker colors denote cities with higher levels of infections and lighter colors denote cities with lower levels of infections in percentiles.

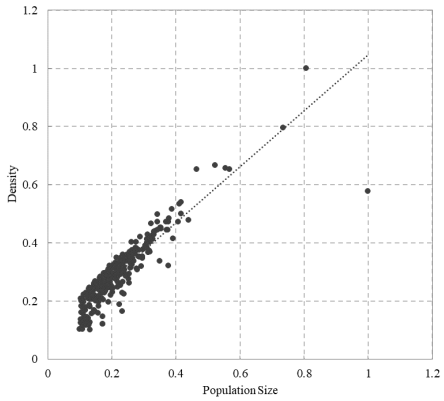

A. Correlation between Population Size and Population Density

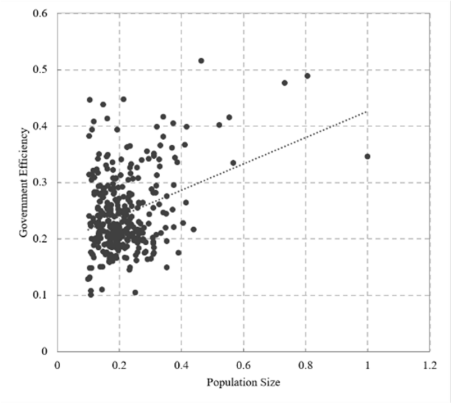

B. Correlation between Population Size and Government Efficiency

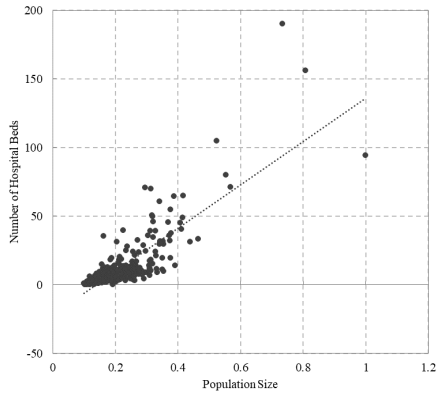

C. Correlation between Population Size and Hospital Beds

FIGURE 2: Correlations between Population Size and City Characteristics

Note: This figure plots the correlations between population size and the three key measures used in our empirical analysis. Population size, density and government efficiency are standardized measures range between [0.1,1]. Hospital beds are measured in 1000.

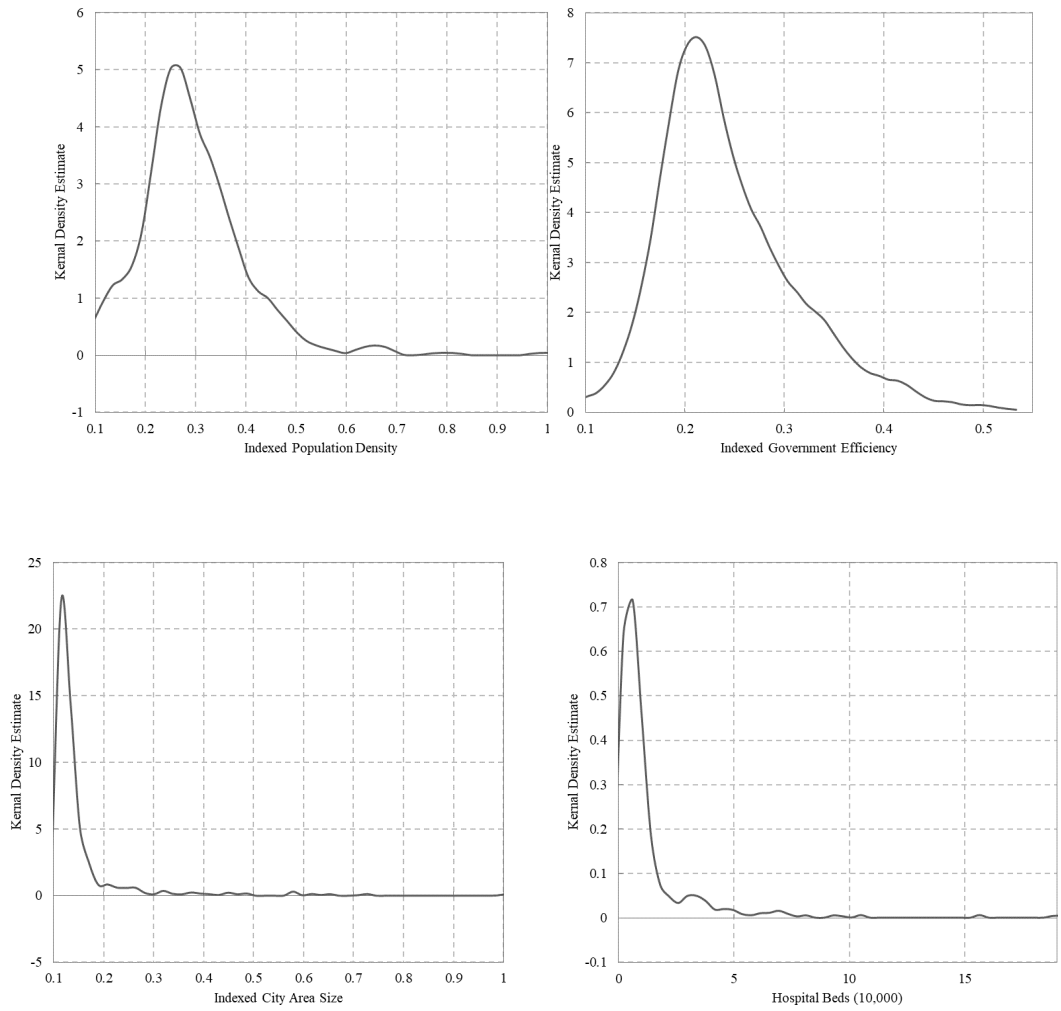

FIGURE 3: Kernel Density of City Attributes

Notes: This figure plots the kernel densities of four city attributes. The four city attributes are the indexed population density (upper left panel), the indexed government efficiency (upper right panel), the indexed city area size (lower left panel), and the number of hospital beds in 10,000 (lower right panel). The kernel density estimates are based on the Epanechnikov kernel.

APPENDIX

This section provides additional information on city level indexes used in our empirical analysis. We obtain city-level measures from the 2019 Global Urban Competitiveness Yearbook. This yearbook was jointly published by Chinese and Foreign Institute of City Competitiveness, Hong Kong Gui Qiang Fang Institute of Global Competitiveness, and World Organization for City Cooperation and Development.

We rely on this data source for our analysis because researchers compiling this yearbook set their main theme as assessing Chinese cities' competitiveness, and one of the key aspects is the government efficiency. The government efficiency index measure is designed to reflect many key aspects of cities in a holistic way. Those aspects include the ability of city residents to generate wealth, the ability of the city government to produce wealth adjusting for the area of the city, and the ability of the city government to manage the city's daily operations efficiently. Overall, it is designed to assess cities' effectiveness in utilizing their resources to maximize wealth.

To compute index measures for different aspects of city competitiveness, researchers collect objective information from various sources which include but are not limited to China City Statistical Yearbook, Educational Statistics Yearbook of China, and Statistical Bulletins from cities' official websites. They also obtain subjective measures through large-scale survey questionnaires. After obtaining the first-hand survey information, they further process the data using Fuzzy Synthetic Evaluation Model to arrive at the final measures. They construct various indicators of cities' competitiveness and carry out professional evaluations to ensure the accuracy and objectiveness of those indicators.

As measures of different aspects of city competitiveness are based on different units, researchers also perform indexation of all measures to arrive at unit-free indicators. Specifically, the following conversion is performed for all measures

$$X_i = \frac{x_i - \min(x)}{\max(x) - \min(x)} \quad \text{(A.1)}$$

where X_i is indicator i's value after indexation, x_i is indicator i's original value, $max(x)$ and $min(x)$ are the maximum and minimum of indicator i's original value in the sample of cities. When an indicator has an original value equal to the minimum in the sample, the value after indexation would be zero. To avoid the confusion with the case when the original value of an indicator is zero, the indexed indicator is further converted into a new indicator, Y_i, that is evenly distributed across $[0.1, 1]$ based on the formula $Y_i = 0.9X_i + 0.1$.[30]

In constructing indicators that summarize various other sub-indicators, such as the government efficiency index, researchers perform a principal component analysis to determine the weight associated with each sub-indicator, and a weighted value is obtained as the aggregate indicator. The government efficiency measure is based on a weighted average of indexed subjective indicators on government capacity, the capacity of law enforcement, transparency of laws and policies, and government organization size. The top three cities with the highest efficiency measures in China in 2018 (published in the 2019 yearbook) are Macao, Hong Kong, and Shenzhen. Because we remove Macao and Hong Kong from our estimation sample and only focus on mainland cities, the maximum value of the government efficiency index is 0.516 as opposed to 1. A similar pattern exists for income per capita since cities with the highest income per capita measures are Taiwan and Hong Kong, which are not included in our sample. Other key indicators published in the same yearbook and used in our analysis are city density, city size, GDP, income per capita, employment size, transport infrastructure index, and human capital index (a city's labor scale and stock adjusted for education). We summarize those measures used in our empirical analysis in Table A1 and report the kernel density estimates for city characteristics in Figure 3. More details can be found in the Yearbook.

[30] Researchers designing the indexation of the measures prefer to differentiate the minimal value of a measure from 0. This monotonic transformation does not impact the estimated coefficients as the additional constant will be absorbed by the dummy variables included in the regression model.

Table A1: Summary Statistics

Variable	Obs	Mean	Std. Dev.	Min	Max
Infections	23,760	1.2361	9.1223	0	424
Death	23,760	0.0296	0.2910	0	9
Density	23,760	0.2932	0.1066	0.1	1
Efficiency	23,760	0.2435	0.0686	0.1	0.516
Num of Beds	23,760	1.2232	1.9230	0	19
Num of Staff	23,760	0.2714	0.8992	0	10
City Size	23,760	0.1524	0.0938	0.1	1
GDP	23,760	0.1736	0.1099	0.1	1
Income per Capita	23,760	0.2407	0.0848	0.1	0.586
Employment	23,760	0.1791	0.1181	0.1	1
Transport Infrastructure	23,760	0.2554	0.1153	0.1	1
Human Capital	23,760	0.2239	0.1528	0.1	1